

Medium effects on the electrical and Hall conductivities of a hot and magnetized pion gas

Pallavi Kalikotay^{1,†}, Snigdha Ghosh^{2,3,*}, Nilanjan Chaudhuri^{4,5,‡}, Pradip Roy^{2,5,§} and Sourav Sarkar^{4,5,¶}

¹*Department of Physics, Kazi Nazrul University, Asansol-713340, West Bengal, India*

²*Saha Institute of Nuclear Physics, 1/AF Bidhannagar, Kolkata-700064, India*

³*Government General Degree College at Kharagpur-II, Madpur, Paschim Medinipur-721149, West Bengal, India*

⁴*Variable Energy Cyclotron Centre, 1/AF Bidhannagar, Kolkata 700064, India*

⁵*Homi Bhabha National Institute, Training School Complex, Anushaktinagar, Mumbai-400085, India*



(Received 8 June 2020; accepted 21 September 2020; published 15 October 2020)

The electrical and Hall conductivities in a uniform magnetic field are evaluated for an interacting pion gas using the kinetic theory approach within the ambit of relaxation time approximation. The in-medium cross sections *vis-à-vis* the relaxation time for $\pi\pi$ scattering are obtained using a one-loop modified thermal propagator for the exchanged ρ and σ mesons using thermal field theoretic techniques. For higher values of the magnetic field, a monotonic increase of the electrical conductivity with the temperature is observed. However, for a given temperature, the conductivity is found to decrease steadily with magnetic field. The Hall conductivity, at lower values of the magnetic field, is found to decrease with the temperature more rapidly than the electrical conductivity, whereas at higher values of the magnetic field, a linear increase is seen. Use of the in-medium scattering cross section is found to produce a significant effect on the temperature dependence of both electrical and Hall conductivities compared to the case where the vacuum cross section is used.

DOI: [10.1103/PhysRevD.102.076007](https://doi.org/10.1103/PhysRevD.102.076007)

I. INTRODUCTION

The study of strongly interacting matter in the presence of a background magnetic field has significant applications in many physical systems (see Ref. [1] for a review). In noncentral heavy ion collisions (HICs) at the RHIC and LHC, strong magnetic fields of the order of $\sim 10^{18}$ G [2,3] or larger may be generated due to the collision geometry. Note that in natural units, 10^{18} G $\approx m_\pi^2 \approx 0.02$ GeV². Thus, the fields produced in HICs are comparable to the QCD scale, i.e., $eB \approx m_\pi^2$, and hence, it can noticeably influence the deconfined medium of quarks and gluons known as quark-gluon plasma (QGP). This has motivated a large number of investigations on the properties of hot and

dense QCD matter in the presence of a background magnetic field in recent times involving several novel and interesting phenomena such as chiral magnetic effect [2,4–6], magnetic catalysis [7–11], and inverse magnetic catalysis [12,13] of dynamical chiral symmetry breaking which may cause significant change in the nature of electroweak [14–17], chiral, and superconducting phase transitions [18–21], electromagnetically induced superconductivity and superfluidity [22,23], and many more. In addition to heavy ion collisions, such magnetic fields of the order of $\sim 10^{15}$ G can also be realized on the surface of certain compact stars called *magnetars*, while in the interior it is estimated to reach magnitudes of the order of $\sim 10^{18}$ G [24–26]. Cosmological model calculations, in fact, predict that during the electroweak phase transition in the early Universe, extremely strong magnetic field as high as $\sim 10^{23}$ G might have been produced [27,28].

The estimation of transport coefficients of relativistic systems in the presence of a magnetic field is important in the context of magnetized neutron stars, cosmology, and relativistic HICs. In the case of HICs, transport coefficients such as the shear and the bulk viscosities and the diffusion coefficients are essential to describe the hydrodynamical evolution of the matter transiently produced in such collisions. In the presence of a magnetic field, this evolution is described by magnetohydrodynamics

*Corresponding author.
snigdha.physics@gmail.com;
snigdha.ghosh@saha.ac.in
†orionpallavi@gmail.com
‡sovon.nilanjan@gmail.com
§pradipk.roy@saha.ac.in
¶sourav@vecc.gov.in

Published by the American Physical Society under the terms of the [Creative Commons Attribution 4.0 International license](https://creativecommons.org/licenses/by/4.0/). Further distribution of this work must maintain attribution to the author(s) and the published article's title, journal citation, and DOI. Funded by SCOAP³.

(MHD), which takes into account the coupling of the magnetic field to the relativistically evolving fluid in a self-consistent way. A good deal of progress has been made in recent times in the evaluation of magnetic-field-dependent transport coefficients such as electrical conductivity [29–36], shear viscosity [35,37–39], the heavy quark diffusion constant [39,40], and the jet quenching parameter [41].

One of the most important transport coefficients required in the formulation of MHD is the electrical conductivity. Also, from a phenomenological point of view, electrical conductivity is important in the sense that if it is large, the created magnetic field in noncentral HICs persists for a longer time [42]. Electrical conductivity of a QGP in a strong magnetic field has been evaluated in Ref. [43] where it was shown that it diverges in the massless limit and is very sensitive to the value of the current quark mass. In Ref. [44], the electrical as well as the Hall conductivities of the QGP have been estimated in a strong magnetic field using a kinetic theory approach as well as the Kubo formalism. It is found that the electrical conductivity decreases in the presence of a magnetic field, especially at a low temperature. Also in Ref. [45], the electrical conductivity of a hot and dense quark matter has been computed in the presence of a magnetic field using kinetic theory beyond the lowest Landau level approximation. It is observed that the transverse electrical conductivity is dominated by the Hall conductivity, and the parallel conductivity has a nominal dependence on both T and μ .

As it was previously mentioned, the produced magnetic field persists for a longer time if the value of electrical conductivity of the medium is large, which is a possibility for the case of QGP. However, as of now it is a general belief that the value of the magnetic field is quite small in hadronic matter (HM) due to the smaller value of the conductivity. As a result, relevant physical quantities calculated in HM will have minor modifications as compared to that in quark matter. In order to substantiate this conjecture, it is necessary to calculate the B -dependent electrical conductivity of HM as accurately as possible taking into account finite temperature and/or density and magnetic field effects. An attempt has been made in Refs. [46,47] to calculate the electrical conductivity of hadron resonance gas (HRG), which has been studied using the relaxation time approximation (RTA) with a constant cross section, whereas in Ref. [48], electrical conductivity along with other transport coefficients of HRG have been computed treating the relaxation time as a free parameter. However, the hadronic phase in HICs attains sufficiently high-temperature ($100 \text{ MeV} \lesssim T \lesssim 155 \text{ MeV}$) and/or high (baryon) density [note that the QGP-hadron phase transition occurs nearly at the temperature $T_c \simeq 155 \text{ MeV}$, which is the (pseudo) critical temperature for the chiral phase transition as obtained in the lattice QCD calculations [49]]. Hence, in order to obtain a more realistic picture, one should incorporate the thermal effects in the cross sections

required to evaluate the transport coefficients which have been ignored in Ref. [47].

In the present work, we intend to evaluate the electrical as well as Hall conductivities of a relativistic pion gas using the kinetic theory approach within the RTA where we incorporate the finite temperature effects in the cross section *vis-à-vis* the relaxation time. We have chosen to calculate the electrical conductivity of pions as they are the most abundant species among the other hadrons produced in the HICs at the RHIC and LHC [50]. This type of study is also important, as the magnetic field produced in heavy ion collisions is of hadronic scale, and hence, the evaluation of transport coefficients of the QGP and the hadronic medium will provide better insight into the time evolution of strongly interacting matter in the presence of a background magnetic field.

The article is organized in the following manner. In the next section, we evaluate the conductivity tensor using the dissipative term obtained from the Boltzmann transport equation (BTE) in the presence of an external magnetic field employing RTA. Section III deals with the evaluation of the relaxation time of pions in thermal medium using an in-medium pionic cross section. In Sec. IV, the numerical results are shown followed by summary and conclusions in Sec. V.

II. ELECTRICAL AND HALL CONDUCTIVITIES FROM KINETIC THEORY

Let us start with the standard expression of the BTE in the presence of an external electromagnetic field [51], which is satisfied by the on-shell single particle phase space distribution function $f_{\pm} = f_{\pm}(t, \vec{r}, \vec{p})$ of the charged pions (π^{\pm}) as

$$\frac{\partial f_{\pm}}{\partial t} + \vec{v} \cdot \frac{\partial f_{\pm}}{\partial \vec{r}} \pm q[\vec{E} + (\vec{v} \times \vec{H})] \cdot \frac{\partial f_{\pm}}{\partial \vec{p}} = C[f_{\pm}], \quad (1)$$

where q is the charge of a proton, $\vec{v} = \vec{p}/\omega_p$ is the velocity, $\omega_p = \sqrt{\vec{p}^2 + m^2}$ is the energy, \vec{E} is the electric field, \vec{H} is the magnetic field, and $C[f]$ denotes the collision kernel. We note that the equilibrium Bose-Einstein distribution function $f_0 = f_0(\omega_p)$ for which $C[f_0] = 0$ is given by

$$f_0(\omega_p) = \frac{1}{e^{\omega_p/T} - 1}, \quad (2)$$

where T is the temperature.

A few comments on the use of the classical dispersion relation $\omega_p = \sqrt{\vec{p}^2 + m^2}$ for the pions are in order here. It is well known that in the presence of an external magnetic field, the momentum states of the charged pions will be Landau quantized and their classical dispersion relation $\omega_p = \sqrt{\vec{p}^2 + m^2}$ with continuous transverse momentum modifies to

$$\omega_{pl} = \sqrt{p_z^2 + (2l+1)qH + m^2}, \quad (3)$$

where l is the Landau level. However, in this work we have ignored the Landau quantization (LQ) in the calculation of the conductivity assuming the magnetic field to be weak. For low values of the external magnetic field, the Landau levels become closely spaced such that the continuum approximation of the transverse momentum of pions holds well. Moreover, we will be using the RTA, where the pion distribution function is assumed to be slightly away from equilibrium, which allows the linearization of the BTE. The use of the RTA implies that the external magnetic field cannot be too high. Finally, the magnitude of the external magnetic field in the hadronic phase of the HIC is usually small, which in turn justifies the use of the weak field approximation in our calculation. A more quantitative analysis of the validity of the continuum approximation will be performed later in Sec. IV.

When the system is out of equilibrium, the dissipative processes within the system try to bring it back to equilibrium. Let us consider the system to be slightly away from equilibrium, which is characterized by the nonequilibrium distribution function $f_{\pm} = f_0 + \delta f_{\pm}$ with $\delta f_{\pm} = -\phi_{\pm} \frac{\partial f_0}{\partial \omega_p} \ll f_0$. As δf_{\pm} is small, the BTE can be linearized.

In order to solve Eq. (1), we treat the right-hand side of Eq. (1) using the RTA and consider only the $2 \rightarrow 2$ scattering process $k + p \rightarrow k' + p'$. In the RTA, the test particle with momentum p is considered to be out of equilibrium, whereas the remaining three particles with momenta k , k' , and p' are in equilibrium. Thus, in the RTA the collision integral in Eq. (1) reduces to [51]

$$C[f_{\pm}] = \frac{\delta f_{\pm}}{\tau} = -\frac{\phi_{\pm}}{\tau} \frac{\partial f_0}{\partial \omega_p}, \quad (4)$$

where τ is the relaxation time. Substituting Eq. (4) into Eq. (1) yields

$$\frac{\partial f_{\pm}}{\partial t} + \vec{v} \cdot \frac{\partial f_{\pm}}{\partial \vec{r}} \pm q[\vec{E} + (\vec{v} \times \vec{H})] \cdot \frac{\partial f_{\pm}}{\partial \vec{p}} = -\frac{\phi_{\pm}}{\tau} \frac{\partial f_0}{\partial \omega_p}. \quad (5)$$

Since we are dealing with a uniform and static medium, both f_{\pm} and f_0 are independent of time and space. Also, the electric field under consideration is very small. Thus, Eq. (5) reduces to

$$\pm q \vec{E} \cdot \vec{v} \frac{\partial f_0}{\partial \omega_p} \pm q(\vec{v} \times \vec{H}) \cdot \frac{\partial \phi_{\pm}}{\partial \vec{p}} \left(\frac{\partial f_0}{\partial \omega_p} \right) = -\frac{\phi_{\pm}}{\tau} \frac{\partial f_0}{\partial \omega_p}. \quad (6)$$

In order to solve for the electrical and Hall conductivities, we take the following ansatz for the functional form of ϕ_{\pm} [33] as

$$\phi_{\pm} = \vec{p} \cdot \vec{\Xi}_{\pm}(\omega_p), \quad (7)$$

where the vector $\vec{\Xi}_{\pm}$ contains information about the dissipation produced due to the electric and magnetic fields and can be expressed most generally as

$$\vec{\Xi}_{\pm} = \alpha_{\pm} \hat{e} + \beta_{\pm} \hat{h} + \gamma_{\pm} (\hat{e} \times \hat{h}), \quad (8)$$

where $\hat{e} = \vec{E}/|\vec{E}|$ and $\hat{h} = \vec{H}/|\vec{H}|$ are the unit vectors along the directions of the electric and magnetic fields, respectively. Substituting Eqs. (7) and (8) into Eq. (6), we get after some simplification

$$\begin{aligned} & \pm \frac{q|\vec{E}|}{\omega_p} (\hat{e} \cdot \vec{p}) \pm \alpha_{\pm} \frac{q|\vec{H}|}{\omega_p} (\hat{e} \times \hat{h}) \cdot \vec{p} \pm \gamma_{\pm} \frac{q|\vec{H}|}{\omega_p} (\hat{e} \cdot \vec{p}) \\ & \pm \gamma_{\pm} \frac{q|\vec{H}|}{\omega_p} (\hat{h} \cdot \vec{p}) (\hat{h} \cdot \hat{e}) \\ & = -\alpha_{\pm} (\hat{e} \cdot \vec{p}) \tau^{-1} - \beta_{\pm} (\hat{h} \cdot \vec{p}) \tau^{-1} - \gamma_{\pm} (\hat{e} \times \hat{h}) \cdot \vec{p} \tau^{-1}. \end{aligned} \quad (9)$$

Comparing the coefficients of $\hat{e} \cdot \vec{p}$, $\hat{e} \times \hat{h}$, and $\hat{h} \cdot \vec{p}$ on both sides of Eq. (9), we obtain

$$\alpha_{\pm} = \pm \frac{q|\vec{E}|}{\omega_p} \frac{\tau}{1 + \omega_c^2 \tau^2}, \quad (10)$$

$$\frac{\beta_{\pm}}{\alpha_{\pm}} = -(\omega_c \tau)^2 (\hat{h} \cdot \hat{e}), \quad (11)$$

$$\frac{\gamma_{\pm}}{\alpha_{\pm}} = -\omega_c \tau, \quad (12)$$

where $\omega_c = |q\vec{H}|/\omega_p$ is the cyclotron frequency. Using Eqs. (10)–(12) in Eq. (8), we can now obtain the vector $\vec{\Xi}_{\pm}$, which in turn is used to get ϕ_{\pm} from Eq. (7) as

$$\begin{aligned} \phi_{\pm} &= \alpha_{\pm} \omega_p \vec{v} \cdot [1 + (\omega_c \tau)^2 (\hat{e} \cdot \hat{h}) \hat{h} - (\omega_c \tau) (\hat{e} \times \hat{h})] \\ &= \pm \frac{q\tau}{1 + (\omega_c \tau)^2} v^i [\delta^{ij} - \omega_c \tau \epsilon^{ijk} h^k + (\omega_c \tau)^2 h^i h^j] E^j, \end{aligned} \quad (13)$$

where the Einstein summation convention has been used.

In order to extract the electrical and Hall conductivities from ϕ_{\pm} , we first note that the macroscopic electrical current density j^i is given by

$$j^i = \sigma^{ij} E^j = \int \frac{d^3 p}{(2\pi)^3} v^i q (\phi_+ - \phi_-) \left(\frac{\partial f_0}{\partial \omega_p} \right). \quad (14)$$

In Eq. (14), σ^{ij} is the conductivity tensor. Now substitution of Eq. (13) into Eq. (14) yields

$$\sigma^{ij} = \delta^{ij} \sigma_0 - \epsilon^{ijk} h^k \sigma_1 + h^i h^j \sigma_2, \quad (15)$$

where

$$\sigma_0 = \frac{gq^2}{3T} \int \frac{d^3 p}{(2\pi)^3} \frac{\vec{p}^2}{\omega_p^2} \frac{\tau}{1 + (\omega_c \tau)^2} f_0(\omega_p) \{1 + f_0(\omega_p)\}, \quad (16)$$

$$\sigma_1 = \frac{gq^2}{3T} \int \frac{d^3 p}{(2\pi)^3} \frac{\vec{p}^2}{\omega_p^2} \frac{\tau(\omega_c \tau)}{1 + (\omega_c \tau)^2} f_0(\omega_p) \{1 + f_0(\omega_p)\}, \quad (17)$$

$$\sigma_2 = \frac{gq^2}{3T} \int \frac{d^3 p}{(2\pi)^3} \frac{\vec{p}^2}{\omega_p^2} \frac{\tau(\omega_c \tau)^2}{1 + (\omega_c \tau)^2} f_0(\omega_p) \{1 + f_0(\omega_p)\}, \quad (18)$$

in which $g = 2$ is the degeneracy of charged pions in the gas since only the charged pions π^+ and π^- participate in the charge conduction. σ_0 is the electrical conductivity in the presence of the magnetic field, σ_1 is the Hall conductivity, and $\sigma_0 + \sigma_2$ is the electrical conductivity in the absence of the external magnetic field. In compact notation, Eqs. (16)–(18) can be written as

$$\sigma_n = \frac{gq^2}{3T} \int \frac{d^3 p}{(2\pi)^3} \frac{\vec{p}^2}{\omega_p^2} \frac{\tau(\omega_c \tau)^n}{1 + (\omega_c \tau)^2} f_0(\omega_p) \{1 + f_0(\omega_p)\}; \quad (19)$$

$n = 0, 1, 2.$

III. THE RELAXATION TIME IN THE MEDIUM

The relaxation time τ which appears in Eq. (19) is the key dynamical input, and for the $2 \rightarrow 2$ process $[\pi(k) + \pi(p) \rightarrow \pi(k') + \pi(p')]$, it is given by [52]

$$[\tau(p)]^{-1} = \frac{g'}{4\omega_p} \iiint \frac{d^3 k}{(2\pi)^3 2\omega_k} \frac{d^3 k'}{(2\pi)^3 2\omega_{k'}} \frac{d^3 p'}{(2\pi)^3 2\omega_{p'}} \times (2\pi)^4 \delta^4(k + p - k' - p') |\mathcal{M}|^2 \times \frac{f_0(\omega_k) \{1 + f_0(\omega_{k'})\} \{1 + f_0(\omega_{p'})\}}{\{1 + f_0(\omega_p)\}}, \quad (20)$$

where the total pion degeneracy $g' = 3$ on account of the fact that both the charged and neutral pions (π^\pm and π^0) participate in the scattering processes via effective strong interaction. Considering $f_0(\omega_{p'}) \simeq f_0(\omega_p)$ and $f_0(\omega_{k'}) \simeq f_0(\omega_k)$ [52], we can integrate over the momenta of the final state particles k' and p' , respectively, obtaining

$$[\tau(p)]^{-1} = \frac{g'}{2} \int \frac{d^3 k}{(2\pi)^3} (\sigma v_{\text{rel}}) f_0(\omega_k) \{1 + f_0(\omega_k)\}, \quad (21)$$

where σ is the total cross section for the $2 \rightarrow 2$ scattering process, and $v_{\text{rel}} = \frac{1}{2\omega_k \omega_p} \lambda^{\frac{1}{2}}((\omega_k + \omega_p)^2, m^2, m^2)$ is the

relative velocity of the initial state particles in which $\lambda(x, y, z) = x^2 + y^2 + z^2 - 2xy - 2yz - 2zx$ is the Källén function.

Let us now proceed to calculate the $\pi\pi$ cross section σ in a thermal medium. The effective interaction of pions with the vector meson ρ and scalar meson σ is given by the following Lagrangian (density) [53]

$$\mathcal{L}_{\text{int}} = g_{\rho\pi\pi} \vec{\rho}_\mu \cdot \vec{\pi} \times \partial^\mu \vec{\pi} + \frac{1}{2} g_{\sigma\pi\pi} m_\sigma \vec{\pi} \cdot \vec{\pi} \sigma, \quad (22)$$

where the coupling constants $g_{\rho\pi\pi} = 6.05$ and $g_{\sigma\pi\pi} = 2.5$ have been obtained from the experimental decay widths of ρ and σ mesons [53,54]. It is now convenient to use the isospin basis so that the invariant amplitudes \mathcal{M}_I for the particular isospin channel with total isospin I are given by [55]

$$\mathcal{M}_2 = g_{\rho\pi\pi}^2 \left[-\left(\frac{s-u}{t-m_\rho^2} \right) - \left(\frac{s-t}{u-m_\rho^2} \right) \right] + 4g_{\sigma\pi\pi}^2 \left[\frac{1}{t-m_\sigma^2} + \frac{1}{u-m_\sigma^2} \right], \quad (23)$$

$$\mathcal{M}_1 = g_{\rho\pi\pi}^2 \left[2 \left(\frac{t-u}{s-m_\rho^2 - \Pi_\rho} \right) + \left(\frac{s-u}{t-m_\rho^2} \right) - \left(\frac{s-t}{u-m_\rho^2} \right) \right] + 4g_{\sigma\pi\pi}^2 \left[\frac{1}{t-m_\sigma^2} - \frac{1}{u-m_\sigma^2} \right], \quad (24)$$

$$\mathcal{M}_0 = g_{\rho\pi\pi}^2 \left[2 \left(\frac{s-u}{t-m_\rho^2} \right) + 2 \left(\frac{s-t}{u-m_\rho^2} \right) \right] + 4g_{\sigma\pi\pi}^2 \left[\frac{3}{s-m_\sigma^2 - \Pi_\sigma} + \frac{1}{t-m_\sigma^2} + \frac{1}{u-m_\sigma^2} \right], \quad (25)$$

where $s = (k+p)^2$, $t = (k-k')^2$, and $u = (k-p')^2$ are the Mandelstam variables, and the vacuum propagators for the ρ and σ in their respective s channels have been replaced by the complete interacting (dressed) propagators obtained from a Dyson-Schwinger sum involving the one-loop in-medium self-energies of ρ and σ denoted by Π_ρ and Π_σ , respectively.

The one-loop self-energies $\Pi_h(q)$ of $h \in \{\rho, \sigma\}$ at finite temperature can be calculated using the standard techniques of real time formalism of finite temperature field theory [54,56]. Contributions to Π_h come from different loop graphs containing other mesons (i, j). The ρ self-energy consists of $\{i, j\} = \{\pi, \pi\}$, $\{\pi, \omega\}$, $\{\pi, h_1\}$, and $\{\pi, a_1\}$ loops, whereas the σ self-energy has a contribution from only $\{i, j\} = \{\pi, \pi\}$ loop. In a general notation, the real part of the self-energy reads

$$\begin{aligned} \text{Re } \Pi_h(q) = & \sum_{\{\pi, j\} \in \{\text{loops}\}} \int \frac{d^3 k}{(2\pi)^3} \frac{1}{2\omega_k \omega_{p_j}} \mathcal{P} \left[\left(\frac{f_0(\omega_k) \omega_{p_j} \mathcal{N}_{\pi_j}^h(k^0 = \omega_k)}{(q_0 - \omega_k)^2 - \omega_{p_j}^2} \right) + \left(\frac{f_0(\omega_k) \omega_{p_j} \mathcal{N}_{\pi_j}^h(k^0 = -\omega_k)}{(q_0 + \omega_k)^2 - \omega_{p_j}^2} \right) \right. \\ & \left. + \left(\frac{f_0(\omega_{p_j}) \omega_k \mathcal{N}_{\pi_j}^h(k^0 = q_0 - \omega_{p_j})}{(q_0 - \omega_{p_j})^2 - \omega_k^2} \right) + \left(\frac{f_0(\omega_{p_j}) \omega_k \mathcal{N}_{\pi_j}^h(k^0 = q_0 + \omega_{p_j})}{(q_0 + \omega_{p_j})^2 - \omega_k^2} \right) \right], \end{aligned} \quad (26)$$

whereas the imaginary part is

$$\begin{aligned} \text{Im } \Pi_h(q) = & -\pi \text{sign}(q_0) \sum_{\{\pi, j\} \in \{\text{loops}\}} \int \frac{d^3 k}{(2\pi)^3} \frac{1}{4\omega_k \omega_{p_j}} \\ & \times \{ [1 + f_0(\omega_k) + f_0(\omega_{p_j})] \{ \mathcal{N}_{\pi_j}^h(k^0 = \omega_k) \delta(q_0 - \omega_k - \omega_{p_j}) - \mathcal{N}_{\pi_j}^h(k^0 = -\omega_k) \delta(q_0 + \omega_k + \omega_{p_j}) \} \\ & - [f_0(\omega_k) - f_0(\omega_{p_j})] \{ \mathcal{N}_{\pi_j}^h(k^0 = \omega_k) \delta(q_0 - \omega_k + \omega_{p_j}) - \mathcal{N}_{\pi_j}^h(k^0 = -\omega_k) \delta(q_0 + \omega_k - \omega_{p_j}) \} \}, \end{aligned} \quad (27)$$

where $\omega_{p_j} = \sqrt{\vec{p}_j^2 + m_j^2}$ with $p_j = (q - k)$. Although the self-energy of ρ contains additional Lorentz indices, in this work we have used the polarization-averaged self-energy of ρ in the expression of the invariant amplitude. It is also to be noted that, corresponding to the loop graphs $\{\pi, h_1\}$ and $\{\pi, a_1\}$ contributing to the self-energy of ρ , Π_ρ has been convoluted with the vacuum spectral functions of the unstable mesons h_1 and a_1 due to their mass uncertainties [57] due to large width. The detailed expressions of \mathcal{N}_{ij}^ρ and \mathcal{N}_{ij}^σ can be found in Ref. [55]. In the expression of the imaginary part of the self-energy, the four terms containing the Dirac delta functions correspond to different physical processes like decay and scattering leading to the absorption of the meson h in the thermal medium.

The isospin-averaged invariant amplitude

$$\overline{|\mathcal{M}|^2} = \sum_I (2I + 1) |\mathcal{M}_I|^2 / \sum_I (2I + 1) \quad (28)$$

is used to obtain the total $\pi\pi \rightarrow \pi\pi$ cross section from

$$\sigma(s) = \frac{1}{64\pi^2 s} \int d\Omega \overline{|\mathcal{M}|^2}. \quad (29)$$

IV. RESULTS AND DISCUSSION

We begin this section by showing the in-medium $\pi\pi \rightarrow \pi\pi$ total cross section as a function of the center-of-mass energy in Fig. 1(a) for different temperatures. At $T = 0$, the cross section obtained using the vacuum self-energies of the ρ and σ mesons is seen to agree with the experimental data [52] shown with red triangles. With the increase in the temperature, the imaginary part of the self-energy increases owing to the in-medium broadening of the resonance spectral functions. Physically, it corresponds to the increase in annihilation probabilities (due to decay and scattering) of ρ and σ in the thermal bath. This in-medium spectral broadening of ρ and σ in turn makes substantial suppression

in the cross section at a high temperature as can be noticed from the figure.

Next, in Fig. 1(b) we have shown the variation of the average relaxation time $\langle \tau \rangle$ of pions with the temperature evaluated using vacuum and in-medium cross sections. Note that the momentum-averaged relaxation time $\langle \tau \rangle$ is obtained from the relation

$$\langle \tau \rangle = \int d^3 p \tau(p) f(\omega_p) / \int d^3 p f(\omega_p). \quad (30)$$

It is seen that the relaxation time obtained using the in-medium cross section is always greater than the same calculated using the vacuum cross section which is also obvious from Eq. (21). Since, the in-medium cross section is suppressed with respect to the vacuum cross section, $\langle \tau \rangle_{\text{vacuum}}$ comes out to be less than $\langle \tau \rangle_{\text{Medium}}$. In order to extract the leading behavior of $\langle \tau \rangle$ as a function of the temperature, we fit the in-medium relaxation time $\langle \tau \rangle_{\text{Medium}}$ with a polynomial function of the form $\sum_{i=0}^3 a_i (\frac{m}{T})^i \frac{1}{T^3}$. This is shown in Fig. 1(c) where we have plotted the fitted function along with $(\frac{a_0}{T^3})$ and $\sum_{i=1}^3 a_i (\frac{m}{T})^i \frac{1}{T^3}$ separately to understand the leading behavior. It is easy to check from Eqs. (21) and (30) that the a_i 's are dimensionful quantities and have the dimensions of the inverse of the cross section, $[\sigma^{-1}]$. It is clearly seen that the leading behavior is well represented by the first term in the fitting function. This can be explained by considering $\langle \tau \rangle \sim 1/(n\sigma)$, where n is the pion density which goes as $n \sim T^3$ in the massless limit and σ is the (T -independent) cross section. The observed deviation from the $1/T^3$ behavior of $\langle \tau \rangle$ at lower and higher temperatures is quite understandable and may be attributed to several factors. Most important among these is the contribution coming from the phase space integrals due to the nonzero pion mass which contain higher inverse powers of T . The T dependence of the cross section can also make a contribution. However, for purposes of discussion, $\langle \tau \rangle$ may well be taken to go as $1/T^3$ in the relevant

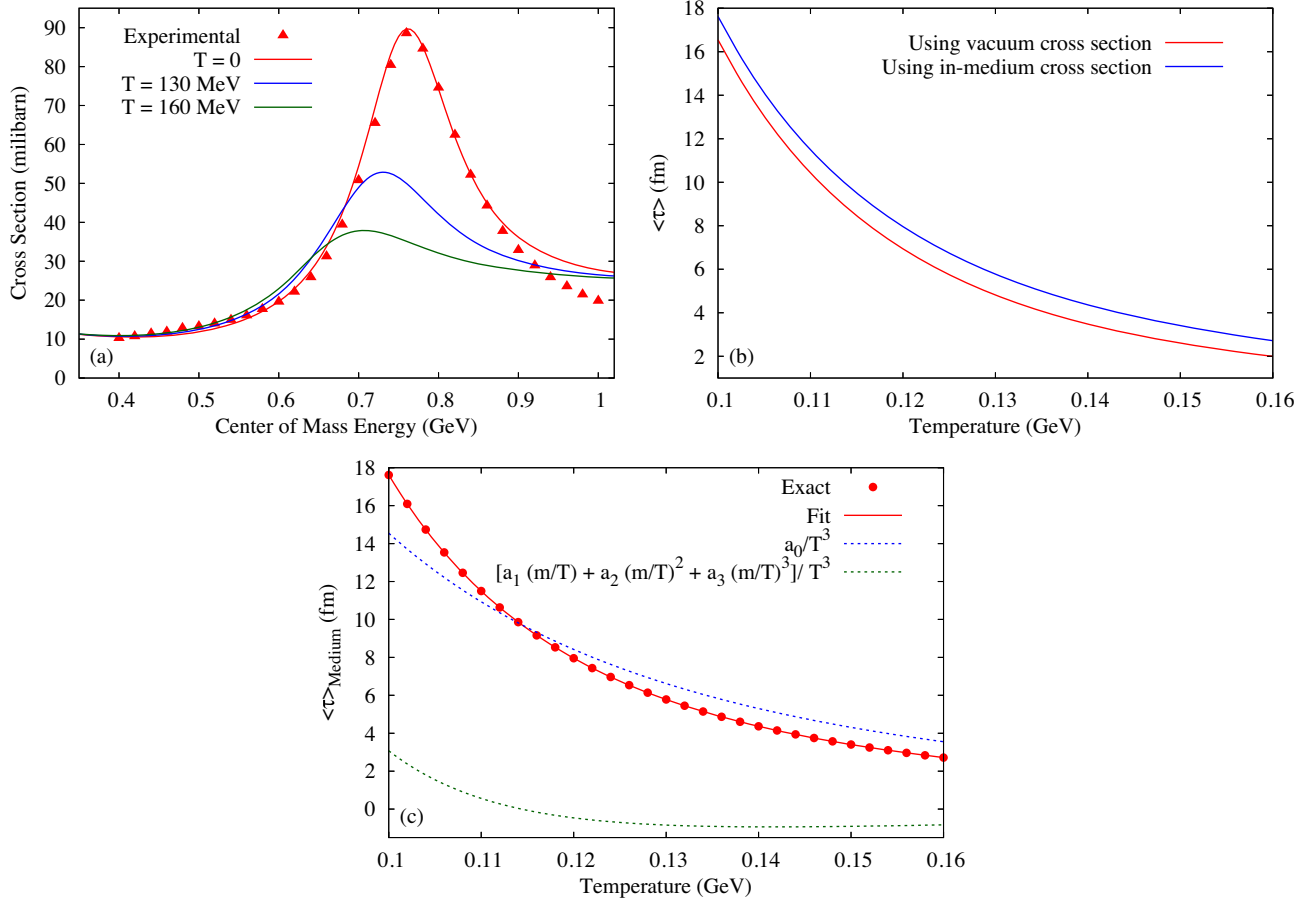


FIG. 1. (a) The variation of the isospin-averaged total $\pi\pi \rightarrow \pi\pi$ cross section as a function of the center-of-mass energy for different temperatures. The experimental data are taken from Ref. [52]. (b) The variation of the average relaxation time $\langle\tau\rangle$ of pions as a function of the temperature calculated using the vacuum and in-medium cross sections. (c) The in-medium $\langle\tau\rangle$ as a function of T fitted with a polynomial function of the form $\sum_{i=0}^3 a_i (\frac{m}{T})^i / T^3$ with $a_0 = 0.0145$ fm GeV³, $a_1 = -0.0109$ fm GeV³, $a_2 = 0.0058$ fm GeV³, and $a_3 = 0.0026$ fm GeV³.

temperature range, and the deviations therefrom will not affect the conclusions significantly.

The variation of σ_0/T as a function of the temperature is shown in Figs. 2(a) and 2(b) for different values of the magnetic field using both the vacuum and in-medium cross sections. To understand the behavior of σ_0/T with the temperature, we first note from Eq. (16) that the temperature dependence of σ_0/T roughly comes from $\sigma_0/T \sim \frac{\tau T}{1+(\omega_c \tau)^2}$. At lower values of the magnetic field, $\omega_c \tau \ll 1$ so that the temperature dependence of τT would dictate the temperature dependence of σ_0/T . We discussed the T dependence of the average relaxation time earlier by fitting a simple function and argued that $\langle\tau\rangle \propto 1/T^3$ is a good approximation in the relevant temperature range. Thus, at lower values of the magnetic field, we expect $\sigma_0/T \sim 1/T^2$, which is quite compatible with Fig. 2(a). The situation is reversed at higher values of the external magnetic field for which $\omega_c \tau \gg 1$, and consequently, the temperature dependence of σ_0/T approximately comes from $\sigma_0/T \sim \frac{T}{\tau} \sim T^4$. We thus expect a monotonically increasing trend of σ_0/T with the

temperature at higher values of the magnetic field as can be noticed in Fig. 2(b). At intermediate values of the magnetic field, we observe a nonmonotonic behavior of σ_0/T with the temperature. In Fig. 2(c), σ_0/T has been plotted as a function of the external magnetic field for different temperatures. Unlike the temperature dependence, σ_0/T has a trivial magnetic field dependence as $\sigma_0/T \sim \frac{1}{1+(\omega_c \tau)^2}$. With the increase in the magnetic field values, the cyclotron frequency ω_c increases linearly so that a monotonically decreasing trend of σ_0/T with external magnetic field is visible in Fig. 2(c). The effect of the in-medium cross section on σ_0/T can be understood similarly from the τ dependence of σ_0/T . As already argued, at a given temperature, for lower values of the magnetic field $\sigma_0/T \sim \tau$, whereas for higher values of the magnetic field $\sigma_0/T \sim 1/\tau$. Since the relaxation time is larger for the in-medium cross section, it is obvious that the use of the in-medium cross section instead of the vacuum cross section will increase (decrease) σ_0/T for lower (higher) values of the external magnetic field. This is clearly observed in Figs. 2(a) and 2(b). This argument also

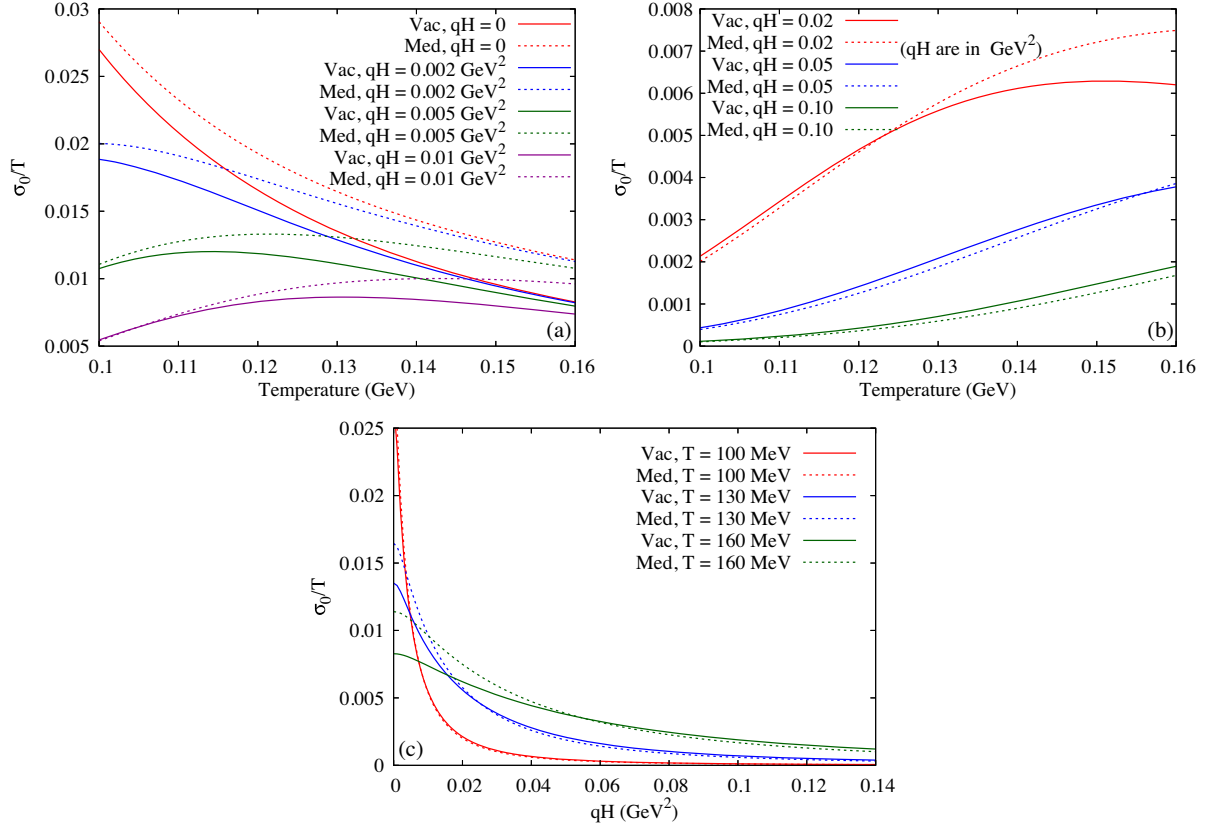


FIG. 2. The variation of σ_0/T (a),(b) as a function of the temperature for different values of the magnetic field strength and (c) as a function of the magnetic field for different values of the temperature. The solid and dashed curves correspond to the estimations of σ_0/T using the vacuum and in-medium cross sections, respectively.

explains the crossing of the dashed curves with the respective solid curves in Fig. 2(c).

Next, in Figs. 3(a) and 3(b), the Hall conductivity scaled with the inverse temperature (σ_1/T) has been depicted as a function of the temperature for different values of the external magnetic field using both the vacuum and in-medium cross sections. The behavior of σ_1/T with the temperature can be understood by a similar analysis as done in the last paragraph. We notice from Eq. (17), the temperature dependence of σ_1/T approximately comes from $\sigma_1/T \sim \frac{\tau^2 T}{1+(\omega_c \tau)^2}$. Therefore, at lower values of the magnetic field, $\omega_c \tau \ll 1$ so that $\sigma_1/T \sim \tau^2 T \sim 1/T^5$. On the other hand, at higher values of the external magnetic field ($\omega_c \tau \gg 1$), the leading temperature dependence of σ_1/T goes as $\sigma_1/T \sim T$. Thus, at lower values of the magnetic field, σ_1/T decreases with the temperature more rapidly than σ_0/T , whereas at higher values of the magnetic field, we notice a linear increase of σ_1/T with the temperature. This also makes σ_1/T to vary nonmonotonically at intermediate values of the external magnetic field as can be noticed in Figs. 3(a) and 3(b). In Fig. 3(c), we have shown σ_1/T as a function of the external magnetic field for different temperatures. The dependence of σ_1/T on the magnetic field goes as $\sigma_1/T \sim \frac{\omega_c}{1+(\omega_c \tau)^2}$, which is basically a

Breit-Wigner function of the magnetic field with peak position $\sim 1/\tau \sim T^3$ and width $\sim \tau \sim 1/T^3$. The Breit-Wigner-like behavior of σ_1/T can be observed in Fig. 3(c) in which the peak position of σ_1/T moves toward higher magnetic field values and the width increases with the temperature. As before, the effect of the in-medium cross section on σ_1/T can be understood from the τ dependence of σ_1/T , i.e., from $\sigma_1/T \sim \frac{\tau^2 \omega_c}{1+(\omega_c \tau)^2}$, which is a monotonically increasing and saturating function of τ . The saturation occurs in the low-temperature (where τ is large) and low magnetic field region in which the overall τ dependence of σ_1/T becomes weaker. Since the in-medium cross section yields a larger relaxation time, the use of the in-medium cross section over the vacuum cross section always increases σ_1/T for any value of the external magnetic field as can be noticed in Figs. 3(a)–3(c). However, in the high magnetic field and low-temperature region, due to the weakening of the τ dependence in σ_1/T , the medium effect in the cross section becomes negligible as one can notice by comparing the separations between the dashed and solid curves of Fig. 3(b) (low-temperature region) and Fig. 3(c) (high magnetic field region).

We now proceed to show the behavior of the quantity σ_2/T as a function of the temperature for different values of

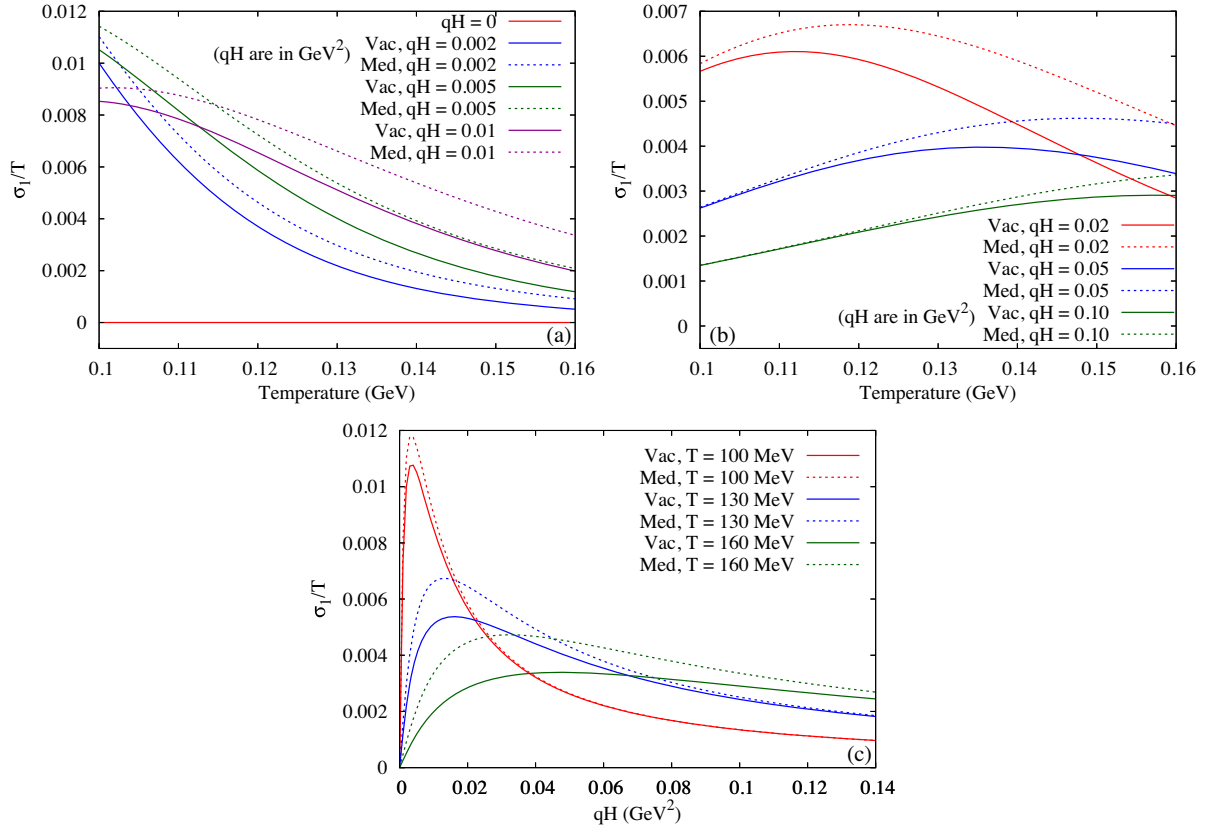


FIG. 3. The variation of σ_1/T (a),(b) as a function of the temperature for different values of the magnetic field strength and (c) as a function of the magnetic field for different values of the temperature. The solid and dashed curves correspond to the estimations of σ_1/T using the vacuum and in-medium cross sections, respectively.

the external magnetic field with both the vacuum and in-medium cross sections in Figs. 4(a) and 4(b). The behavior of σ_2/T with the temperature can be analogously understood from Eq. (18) in which the temperature dependence of σ_2/T approximately goes as $\sigma_2/T \sim \frac{\tau^3 T}{1+(\omega_c \tau)^2}$. Therefore, at lower values of the magnetic field ($\omega_c \tau \ll 1$), $\sigma_2/T \sim \tau^3 T \sim 1/T^8$. On the other hand, at higher values of the external magnetic field ($\omega_c \tau \gg 1$), the leading temperature dependence of σ_2/T is approximately given by $\sigma_2/T \sim \tau \sim 1/T^3$. Thus, σ_2/T always decreases monotonically with the increase in the temperature even more rapidly than σ_1/T in all values of the magnetic field considered here [see Figs. 4(a) and 4(b)]. Next, in Fig. 4(c), the magnetic field dependence of σ_2/T has been depicted for different temperatures. σ_2/T depends on the magnetic field as $\sigma_2/T \sim \frac{(\omega_c \tau)^2}{1+(\omega_c \tau)^2}$, which is a monotonically increasing and saturating function of the magnetic field, thus explaining the analogous behavior of the curves in the figure. To understand the effect of the in-medium cross section on σ_2/T , we first note that the τ dependence of σ_2/T is given by $\sigma_2/T \sim \frac{\tau^3 \omega_c^2}{1+(\omega_c \tau)^2}$ which is a monotonically increasing function of τ for a particular value of the magnetic field. The rate of increase is more for higher magnetic field values. Thus, we notice from Figs. 4(a)–4(c)

that the use of the in-medium cross section over the vacuum cross section always increases σ_2/T for the values of the magnetic field considered here. Moreover, at higher values of the external magnetic field, due to the increase of τ dependence in σ_2/T , the medium effects become more significant, as can be observed by comparing the separations between the dashed and solid curves of Figs. 4(a)–4(c).

Finally, we note that the normalized ratio $\frac{\sigma_0}{\sigma_0+\sigma_2}$ could be a measure of the anisotropy brought in by the external magnetic field since the quantity $\sigma_0 + \sigma_2$ is the electrical conductivity in the absence of the magnetic field. We therefore plot $\frac{\sigma_0}{\sigma_0+\sigma_2}$ as a function of the temperature and magnetic field in Figs. 5(a)–5(c). With the increase in the temperature, the ratio increases toward its asymptotic value 1, whereas with the increase in the magnetic field, the ratio rapidly decreases from 1. Physically, it corresponds to the fact that the magnetic field tries to bring anisotropy in the medium, whereas the thermal fluctuation tries to diminish it. Moreover, comparing the solid and dashed curves in Figs. 5(a)–5(c), we find that the use of medium effects in the cross section makes the system more anisotropic in the presence of the external magnetic field.

We have already mentioned in Sec. II that we are neglecting the LQ of the charged pion dispersion relation [see Eq. (3)] while calculating the conductivities. However,

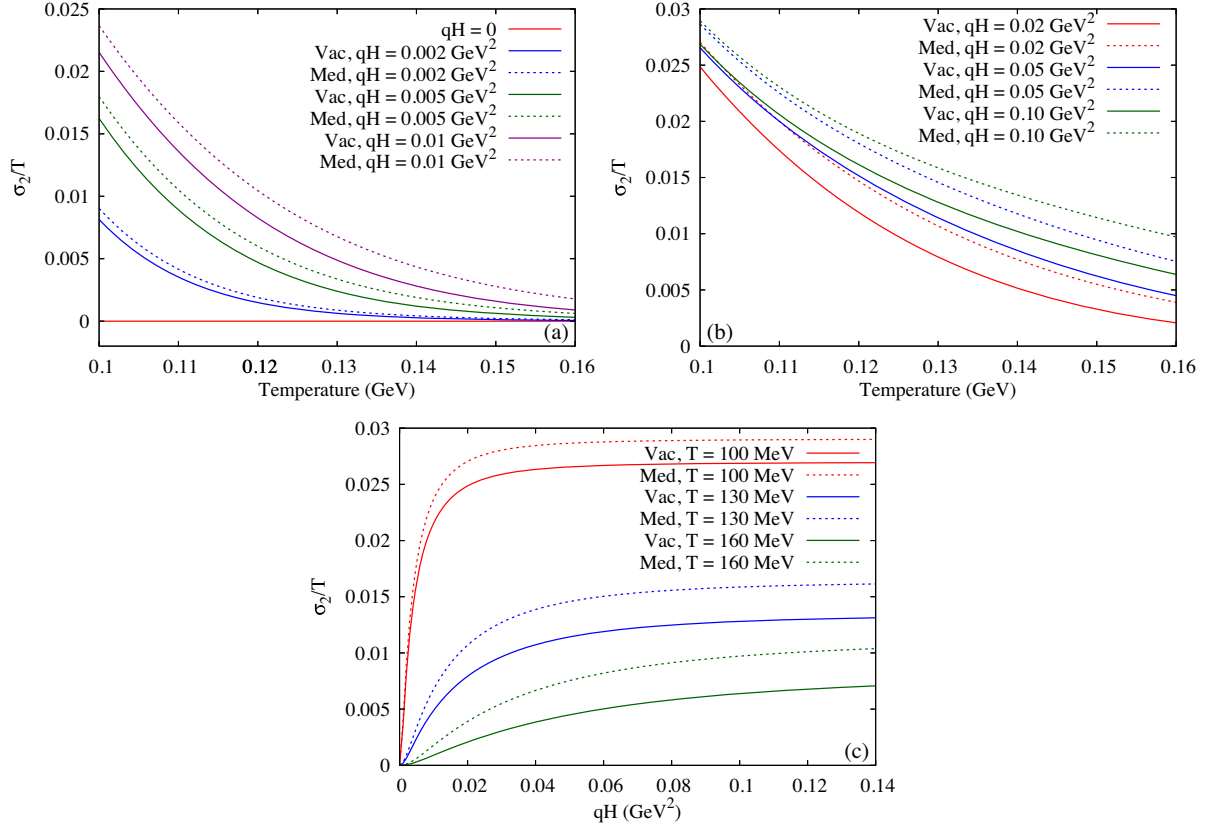


FIG. 4. The variation of σ_2/T (a),(b) as a function of the temperature for different values of the magnetic field strength and (c) as a function of the magnetic field for different values of the temperature. The solid and dashed curves correspond to the estimations of σ_2/T using the vacuum and in-medium cross sections, respectively.

to check the validity of this continuum approximation, let us now calculate the conductivities incorporating the LQ of the pion transverse momentum. To a first approximation, the LQ can be incorporated in the final expression of the conductivities in Eq. (19) by the following replacements:

$$\omega_p \rightarrow \omega_{pl} = \sqrt{p_z^2 + (2l+1)qH + m^2}, \quad (31)$$

$$|\vec{p}| \rightarrow \sqrt{p_z^2 + (2l+1)qH}, \quad (32)$$

$$\int \frac{d^3p}{(2\pi)^3} \rightarrow \frac{qH}{2\pi} \sum_{l=0}^{\infty} \int_{-\infty}^{\infty} \frac{dp_z}{2\pi}, \quad (33)$$

so that the conductivities with LQ become

$$\begin{aligned} \sigma_n^{\text{LQ}} &= \frac{gq^2 qH}{3T} \frac{1}{2\pi} \sum_{l=0}^{\infty} \int_{-\infty}^{\infty} \frac{dp_z}{2\pi} \frac{p_z^2 + (2l+1)qH}{\omega_{pl}^2} \frac{\tau(\omega_{c,l}\tau)^n}{1 + (\omega_{c,l}\tau)^2} \\ &\times f_0(\omega_{pl}) \{1 + f_0(\omega_{pl})\}; \quad n = 0, 1, 2, \end{aligned} \quad (34)$$

where $\omega_{c,l} = qH/\omega_{pl}$. In Fig. 6, we have shown the ratio $\sigma_n^{\text{LQ}}/\sigma_n$ as a function of the external magnetic field at $T = 130$ MeV. From the figure, we can see that in the low magnetic field region ($qH \lesssim m^2$), the ratios are almost

unity, which implies that the use of the continuum approximation is well justified in the weak field region. However, for higher magnetic field values, the continuum approximation breaks down and the LQ becomes important. For example, at $qH = 0.10$ GeV², LQ modifies the values of σ_0 and σ_1 by less than 5%, whereas the change in σ_2 is about 30%. Therefore, even if we have shown numerical results for a wider range of magnetic field values ($0 \leq qH \leq 0.1$ GeV²) neglecting the LQ, our results are strictly valid for the weak magnetic field ($0 \leq qH < m^2$) likely to be realized in the hadronic phase of a HIC.

In Fig. 7(a), we have made a comparison of the electrical conductivity obtained in this work with the other available estimations in the literature. We see that our estimation of electrical conductivity at zero magnetic field agrees well with the earlier estimations by Grief *et al.* [58] and Fernandez-Fraile and Nicola [59], whereas it does not agree well with the lattice QCD estimation [60]. Also, our result at $qH = 0.02$ GeV² is lower than the values obtained by Feng [44] for a system of relativistic quark-gluon gas. This is expected, as the conductivity of QGP is much larger than that of hadron gas. Finally, our result at $qH = 0.05$ GeV² is in good qualitative and quantitative agreement with the result of Das *et al.* [47] calculated for hadron resonance gas.

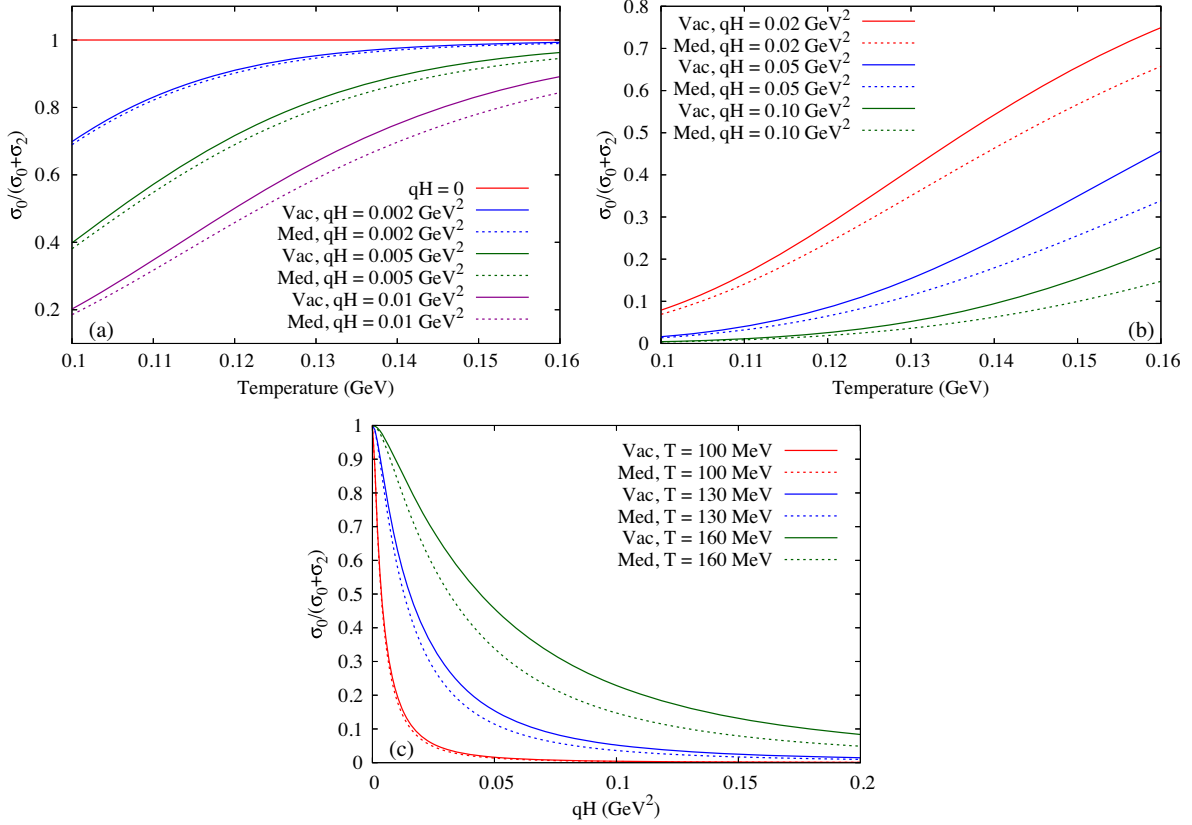


FIG. 5. The variation of the anisotropy measure $\frac{\sigma_0}{\sigma_0+\sigma_2}$ (a),(b) as a function of the temperature for different values of the magnetic field strength and (c) as a function of the magnetic field for different values of the temperature. The solid and dashed curves correspond to the estimations of $\frac{\sigma_0}{\sigma_0+\sigma_2}$ using the vacuum and in-medium cross sections, respectively.

We have already mentioned in Sec. I that a sufficiently high value of electrical conductivity of the medium can sustain the rapidly decaying magnetic field in a HIC [3,38,42,61]. To see how our estimated electrical conductivity (for a system of pion gas) modifies the decay of the magnetic field in HIC, we have calculated the time (t) dependence of the maximum value of the magnetic field

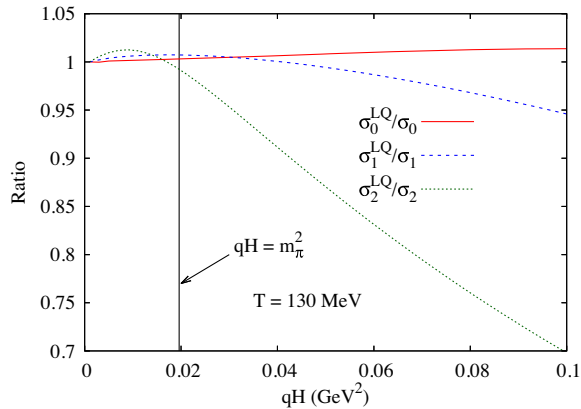


FIG. 6. The ratio σ_n^{LQ}/σ_n as a function of the external magnetic field at $T = 130$ MeV. The solid black vertical line corresponds to $qH = m_\pi^2$. Up to 300 Landau levels are taken into consideration.

for a peripheral Au + Au collision at the RHIC energy ($\sqrt{s} = 200$ GeV) using the simplified expression used by Tuchin [38] for a static medium. In Fig. 7(b), we have plotted the decay of the maximum magnetic field value in the peripheral Au + Au collision at the RHIC for different values of electrical conductivities. In our calculation, we have obtained a maximum value of σ_0 as 3 MeV, whereas in a QGP medium it has typical value of ≈ 15 MeV [42, 61–63]. From the figure, it can be noticed that for a constant $\sigma_0 = 15$ MeV throughout the evolution, a magnetic field value of the order of 10^{-4} GeV² is sustained even at $t = 10$ fm. But if we consider the constant $\sigma_0 = 1$ –3 MeV (as obtained in the current work for a pion gas) throughout the evolution, the sustained value of the magnetic field at $t = 10$ fm is of the order of 10^{-5} GeV². In reality, electrical conductivity is not expected to be constant throughout the evolution. In the early stage (QGP phase), σ_0 will be large (~ 15 MeV), and in the later stages (hadronic phase), σ_0 will be small (~ 5 MeV). Therefore, the time evolution of the actual magnetic field value is expected to lie in between the violet and green curves in the figure. Moreover, in Fig. 7(b), we have considered a medium with no hydrodynamic expansion for the estimation of the decay of magnetic field. For an expanding medium (which is the more realistic scenario for HIC), the magnetic field will

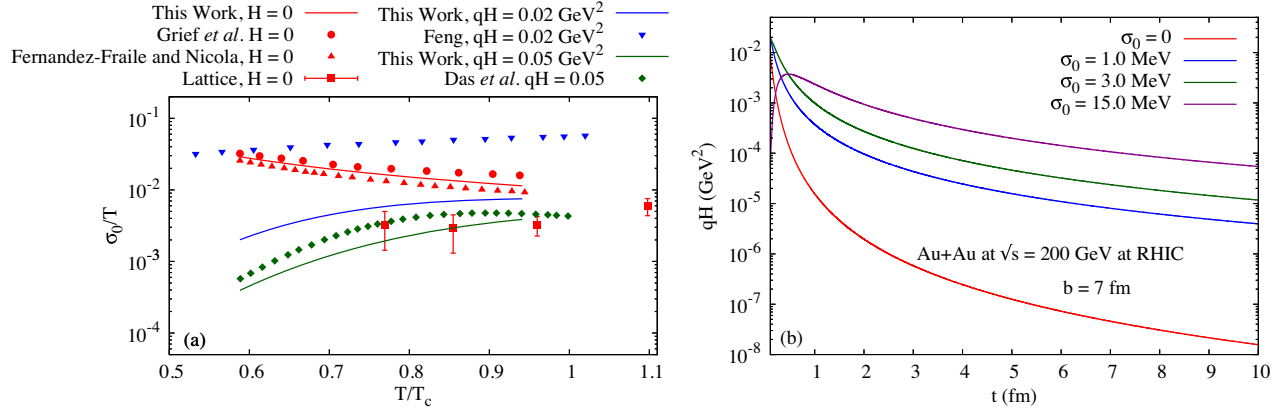


FIG. 7. (a) The comparison of σ_0/T at zero magnetic field with Grief *et al.* [58], Fernandez-Fraile and Nicola [59], and lattice QCD calculation [60] and at nonzero magnetic field with Feng [44] and Das *et al.* [47]. (b) The decay of the maximum magnetic field value in peripheral Au + Au collision at the RHIC for different values of electrical conductivities.

sustain for a longer period as shown in Ref. [38]. Thus, we can conclude that a weak magnetic field can be present in the later stages of HIC and could be phenomenologically relevant.

V. SUMMARY AND CONCLUSIONS

We have evaluated the conductivity tensor using the Boltzmann transport equation in a magnetic field and hence evaluated the electrical conductivity, Hall conductivity, and σ_2 for a system consisting of a pion gas. The information pertaining to the pion gas enters through the relaxation time into the expression of the three conductivities. The $\pi\pi$ cross section has been calculated in a thermal medium using the real time formalism of finite temperature field theory. We have shown the variation of these three conductivities with the temperature for different values of the magnetic field. It has been observed that electrical conductivity and Hall conductivity are very sensitive to the magnetic field strength and the in-medium cross sections. Moreover, as we have not considered the LQ in the dispersion relation of charged pions, our results are more accurate in the low magnetic field values ($qH \lesssim m^2$), which is the realistic scenario for the later stages of HICs.

Both the electrical and Hall conductivities have been found to increase with temperature for a given value of the magnetic field when the in-medium cross section is used. For a given temperature, there is no appreciable change (except at lower B) in the electrical conductivity with the magnetic field when the medium-dependent cross section is used. A more detailed observation shows a monotonically increasing trend of electrical conductivity with the increase in the temperature at higher values of the magnetic field. However, for a given temperature, the conductivity has been found to decrease monotonically as a function of the

magnetic field. In the case of Hall conductivity, it has been found that at lower values of the magnetic field, it decreases with the increase in the temperature more rapidly than the electrical conductivity, whereas at higher values of the magnetic field, a linear increase of the Hall conductivity with the temperature has been observed. For a given temperature, as long as it is low we have seen a Breit-Wigner-type structure in the Hall conductivity as a function of the magnetic field. This structure disappears and tends to saturate at a higher temperature. This behavior can be attributed to the substantial spectral broadening of the exchanged particle at a high temperature.

The electrical conductivity obtained in this work has been shown to have both qualitative and quantitative agreement with earlier estimates available in the literature. Moreover, the calculated electrical conductivity has been shown to be sufficient for causing a significant delay in the decay of the external magnetic field in a HIC. This leads to the conclusion that, a weak magnetic field can be present in the later stage of a HIC (in hadronic phase) and could be phenomenologically relevant.

Finally, we should mention that we have included only pions in our calculations as they are more abundantly produced in the temperature range achievable in HICs. Hadrons heavier than the pion can, in principle, be included, as is done in Ref. [47] using a constant cross section. However, in the present formalism it will be extremely nontrivial to solve the coupled transport equations as well as to calculate a plethora of cross sections due to the inclusion of multiple species.

ACKNOWLEDGMENTS

The authors are funded by the Department of Atomic Energy, Government of India.

- [1] *Strongly Interacting Matter in Magnetic Fields*, edited by D. Kharzeev, K. Landsteiner, A. Schmitt, and H.-U. Yee (Springer, Heidelberg, 2013), Vol. 871.
- [2] D. E. Kharzeev, L. D. McLerran, and H. J. Warringa, *Nucl. Phys. A* **803**, 227 (2008).
- [3] V. Skokov, A. Illarionov, and V. Toneev, *Int. J. Mod. Phys. A* **24**, 5925 (2009).
- [4] K. Fukushima, D. E. Kharzeev, and H. J. Warringa, *Phys. Rev. D* **78**, 074033 (2008).
- [5] D. E. Kharzeev and H. J. Warringa, *Phys. Rev. D* **80**, 034028 (2009).
- [6] G. Bali, F. Bruckmann, G. Endrodi, Z. Fodor, S. Katz, S. Krieg, A. Schafer, and K. Szabo, *J. High Energy Phys.* **02** (2012) 044.
- [7] I. A. Shovkovy, in *Strongly Interacting Matter in Magnetic Fields*, edited by D. Kharzeev, K. Landsteiner, A. Schmitt, and H.-U. Yee, Lecture Notes in Physics Vol. 871 (Springer, Berlin, 2013), pp. 13–49.
- [8] V. Gusynin, V. Miransky, and I. Shovkovy, *Phys. Rev. Lett.* **73**, 3499 (1994); **76**, 1005(E) (1996).
- [9] V. Gusynin, V. Miransky, and I. Shovkovy, *Phys. Rev. D* **52**, 4718 (1995).
- [10] V. Gusynin, V. Miransky, and I. Shovkovy, *Nucl. Phys. B* **462**, 249 (1996).
- [11] V. Gusynin, V. Miransky, and I. Shovkovy, *Nucl. Phys. B* **563**, 361 (1999).
- [12] F. Preis, A. Rebhan, and A. Schmitt, *J. High Energy Phys.* **03** (2011) 033.
- [13] F. Preis, A. Rebhan, and A. Schmitt, in *Strongly Interacting Matter in Magnetic Fields*, edited by D. Kharzeev, K. Landsteiner, A. Schmitt, and H. U. Yee, Lecture Notes in Physics Vol. 871 (Springer, Berlin, 2013), pp. 51–86.
- [14] P. Elmfors, K. Enqvist, and K. Kainulainen, *Phys. Lett. B* **440**, 269 (1998).
- [15] V. Skalozub and M. Bordag, *Int. J. Mod. Phys. A* **15**, 349 (2000).
- [16] N. Sadooghi and K. Anaraki, *Phys. Rev. D* **78**, 125019 (2008).
- [17] J. Navarro, A. Sanchez, M. E. Tejada-Yeomans, A. Ayala, and G. Piccinelli, *Phys. Rev. D* **82**, 123007 (2010).
- [18] S. Fayazbakhsh and N. Sadooghi, *Phys. Rev. D* **82**, 045010 (2010).
- [19] S. Fayazbakhsh and N. Sadooghi, *Phys. Rev. D* **83**, 025026 (2011).
- [20] V. Skokov, *Phys. Rev. D* **85**, 034026 (2012).
- [21] K. Fukushima and J. M. Pawłowski, *Phys. Rev. D* **86**, 076013 (2012).
- [22] M. Chernodub, *Phys. Rev. Lett.* **106**, 142003 (2011).
- [23] M. Chernodub, J. Van Doorselaere, and H. Verschelde, *Phys. Rev. D* **85**, 045002 (2012).
- [24] R. C. Duncan and C. Thompson, *Astrophys. J.* **392**, L9 (1992).
- [25] C. Thompson and R. C. Duncan, *Astrophys. J.* **408**, 194 (1993).
- [26] D. Lai and S. L. Shapiro, *Astrophys. J.* **383**, 745 (1991).
- [27] T. Vachaspati, *Phys. Lett. B* **265**, 258 (1991).
- [28] L. Campanelli, *Phys. Rev. Lett.* **111**, 061301 (2013).
- [29] P. Buividovich, M. Chernodub, D. Kharzeev, T. Kalaydzhyan, E. Luschevskaya, and M. Polikarpov, *Phys. Rev. Lett.* **105**, 132001 (2010).
- [30] S. Pu, S.-Y. Wu, and D.-L. Yang, *Phys. Rev. D* **91**, 025011 (2015).
- [31] D. Satow, *Phys. Rev. D* **90**, 034018 (2014).
- [32] E. Gorbar, I. Shovkovy, S. Vilchinskii, I. Rudenok, A. Boyarsky, and O. Ruchayskiy, *Phys. Rev. D* **93**, 105028 (2016).
- [33] A. Harutyunyan and A. Sedrakian, *Phys. Rev. C* **94**, 025805 (2016).
- [34] B. Kerbikov and M. Andreichikov, *Phys. Rev. D* **91**, 074010 (2015).
- [35] M. G. Alford, H. Nishimura, and A. Sedrakian, *Phys. Rev. C* **90**, 055205 (2014).
- [36] S.-i. Nam, *Phys. Rev. D* **86**, 033014 (2012).
- [37] X.-G. Huang, A. Sedrakian, and D. H. Rischke, *Ann. Phys. (Amsterdam)* **326**, 3075 (2011).
- [38] K. Tuchin, *Adv. High Energy Phys.* **2013**, 490495 (2013).
- [39] S. I. Finazzo, R. Critelli, R. Rougemont, and J. Noronha, *Phys. Rev. D* **94**, 054020 (2016); **96**, 019903(E) (2017).
- [40] K. Fukushima, K. Hattori, H.-U. Yee, and Y. Yin, *Phys. Rev. D* **93**, 074028 (2016).
- [41] S. Li, K. A. Mamo, and H.-U. Yee, *Phys. Rev. D* **94**, 085016 (2016).
- [42] U. Gursoy, D. Kharzeev, and K. Rajagopal, *Phys. Rev. C* **89**, 054905 (2014).
- [43] K. Hattori and D. Satow, *Phys. Rev. D* **94**, 114032 (2016).
- [44] B. Feng, *Phys. Rev. D* **96**, 036009 (2017).
- [45] K. Fukushima and Y. Hidaka, *Phys. Rev. Lett.* **120**, 162301 (2018).
- [46] A. Das, H. Mishra, and R. K. Mohapatra, *Phys. Rev. D* **100**, 114004 (2019).
- [47] A. Das, H. Mishra, and R. K. Mohapatra, *Phys. Rev. D* **99**, 094031 (2019).
- [48] A. Dash, S. Samanta, J. Dey, U. Gangopadhyaya, S. Ghosh, and V. Roy, *Phys. Rev. D* **102**, 016016 (2020).
- [49] A. Bazavov *et al.* (HotQCD Collaboration), *Phys. Rev. D* **90**, 094503 (2014).
- [50] *The Physics of the Quark-Gluon Plasma*, edited by S. Sarkar, H. Satz, and B. Sinha (Springer, Heidelberg, 2010), Vol. 785.
- [51] S. De Groot, in *Relativistic Kinetic Theory. Principles and Applications*, edited by W. Van Leeuwen and C. Van Weert (North-Holland Publishing Company, Amsterdam, 1980).
- [52] M. Prakash, M. Prakash, R. Venugopalan, and G. Welke, *Phys. Rep.* **227**, 321 (1993).
- [53] O. Krehl, C. Hanhart, S. Krewald, and J. Speth, *Phys. Rev. C* **62**, 025207 (2000).
- [54] S. Mallik and S. Sarkar, *Hadrons at Finite Temperature* (Cambridge University Press, Cambridge, England, 2016).
- [55] S. Mitra, S. Ghosh, and S. Sarkar, *Phys. Rev. C* **85**, 064917 (2012).
- [56] M. L. Bellac, *Thermal Field Theory*, Cambridge Monographs on Mathematical Physics (Cambridge University Press, Cambridge, England, 2011).
- [57] S. Sarkar, E. Oset, and M. Vicente Vacas, *Nucl. Phys. A* **750**, 294 (2005); **780**, 90(E) (2006).
- [58] M. Greif, C. Greiner, and G. S. Denicol, *Phys. Rev. D* **93**, 096012 (2016); **96**, 059902(E) (2017).
- [59] D. Fernandez-Fraile and A. Gomez Nicola, *Phys. Rev. D* **73**, 045025 (2006).

- [60] A. Amato, G. Aarts, C. Allton, P. Giudice, S. Hands, and J.-I. Skullerud, *Phys. Rev. Lett.* **111**, 172001 (2013).
- [61] K. Tuchin, *Phys. Rev. C* **82**, 034904 (2010); **83**, 039903(E) (2011).
- [62] H.-T. Ding, A. Francis, O. Kaczmarek, F. Karsch, E. Laermann, and W. Soeldner, *Phys. Rev. D* **83**, 034504 (2011).
- [63] G. Aarts, C. Allton, J. Foley, S. Hands, and S. Kim, *Phys. Rev. Lett.* **99**, 022002 (2007).